JOURNAL OF VIROLOGY, Sept. 1996, p. 6358–6369 Vol. 70, No. 9
0022-538X/96/$04.00+0

Prolonged Gene Expression and Cell Survival after Infection by a Herpes Simplex Virus Mutant Defective in the Immediate-Early Genes Encoding ICP4, ICP27, and ICP22

NAXIN WU,[1] SIMON C. WATKINS,[2] PRISCILLA A. SCHAFFER,[3] AND NEAL A. DELUCA[1]*

Department of Molecular Genetics and Biochemistry[1] and Department of Cell Biology and Physiology,[2] University of Pittsburgh School of Medicine, Pittsburgh, Pennsylvania 15261, and Division of Molecular Genetics, Dana-Farber Cancer Institute, and Department of Microbiology and Molecular Genetics, Harvard Medical School, Boston, Massachusetts 02115[3]

Received 19 March 1996/Accepted 21 May 1996

Very early in infection, herpes simplex virus (HSV) expresses four immediate-early (IE) regulatory proteins, ICP4, ICP0, ICP22, and ICP27. The systematic inactivation of sets of the IE proteins in *cis*, and the subsequent phenotypic analysis of the resulting mutants, should provide insights into how these proteins function in the HSV life cycle and also into the specific macromolecular events that are altered or perturbed in cells infected with virus strains blocked very early in infection. This approach may also provide a rational basis to assess the efficacy and safety of HSV mutants for use in gene transfer experiments. In this study, we generated and examined the phenotype of an HSV mutant simultaneously mutated in the ICP4, ICP27, and ICP22 genes of HSV. Unlike mutants deficient in ICP4 (*d*120), ICP4 and ICP27 (*d*92), and ICP4 and ICP22 (*d*96), mutants defective in ICP4, ICP27, and ICP22 (*d*95) were visually much less toxic to Vero and human embryonic lung cells. Cells infected with *d*95 at a multiplicity of infection of 10 PFU per cell retained a relatively normal morphology and expressed genes from the viral and cellular genomes for at least 3 days postinfection. The other mutant backgrounds were too toxic to allow examination of gene expression past 1 day postinfection. However, when cell survival was measured by the capacity of the infected cells to form colonies, *d*95 inhibited colony formation similarly to *d*92. This apparent paradox was reconciled by the observation that host cell DNA synthesis was inhibited in cells infected with *d*120, *d*92, *d*96, and *d*95. In addition, all of the mutants exhibited pronounced and distinctive alterations in nuclear morphology, as determined by electron microscopy. The appearance of *d*95-infected cells deviated from that of uninfected cells in that large circular structures formed in the nucleus. *d*95-infected cells abundantly expressed ICP0, which accumulated in fine punctate structures in the nucleus at early times postinfection and coalesced or grew to the large circular objects that were revealed by electron microscopy. Therefore, while the abundant accumulation of ICP0 in the absence of ICP4, ICP22, and ICP27 may allow for prolonged gene expression, cell survival is impaired, in part, as a result of the inhibition of cellular DNA synthesis.

The more than 75 genes of herpes simplex virus type 1 (HSV-1) (40, 41) are expressed in a regulated and sequential manner such that three broad categories of genes, immediate-early (IE), early (E), and late (L), can be defined (26, 27). The five genes classically designated IE genes are expressed shortly after the genome arrives in the nucleus and in the absence of prior de novo viral protein synthesis (26, 27). Transcription of the IE genes is activated by the virion protein VP16 (3, 8), which functions as a complex on IE promoters with cellular Oct1 and other host cell proteins (19–21, 33, 46, 71). The IE genes encode the proteins infected cell polypeptide 4 (ICP4), ICP27, ICP0, ICP22, and ICP47 (10, 26, 50, 74).

ICP4, ICP0, ICP27, and ICP22 are nuclear phosphoproteins (50, 77) and possess regulatory activities which are thought to prime the cell for, and participate in, the efficient cascade of subsequent viral gene expression, DNA replication, and the production of progeny virions. ICP4 is a large multifunctional protein. It can act as a transcription factor that either represses (12, 22, 45, 48, 56) or activates (12, 16, 18, 47, 53) transcription through contacts with the general transcriptional machinery (22, 67). ICP4 is largely responsible for the transition from the IE to E phase of viral gene expression (14, 52, 73). ICP0 will activate most test promoters in transient assays (16, 18, 47, 53) and has been found to elevate levels of viral gene expression and growth in tissue culture and in the trigeminal ganglia of mice (6, 7, 37). It also facilitates the reactivation of virus from latency in the mouse model (6, 37). ICP27 also appears to be multifunctional. Several studies have shown that it can modulate the activity of ICP4 and ICP0 (44, 54, 66), as well as the modification state of ICP4 (44, 54, 70). ICP27 has also been shown to regulate viral and cellular mRNA processing events (9, 23, 24, 42, 43, 61–63, 68). The combined activities of ICP27 contribute to efficient DNA replication and late gene expression (39, 57); however, recent studies have shown that ICP27 also significantly contributes to elevated levels of early gene expression (59, 72). The contribution of ICP27 to the elevated levels of some early proteins has provided an explanation for the requirement for ICP27 for viral DNA replication (72). ICP22 is not essential for growth in many cell types, including Vero cells, and acts to promote efficient late gene expression in a cell-type-dependent manner (65). It has also been shown to be involved in the production of a novel modified form of RNA polymerase II (55). How all four of these proteins function together to orchestrate the regulatory cascade seen in HSV-infected cells remains to be determined. Additionally, the effects of these proteins on host cell metabolism are unknown.

In the absence of ICP4, only the remaining IE proteins,

* Corresponding author. Mailing address: E1257 Biomedical Science Tower, Department of Molecular Genetics and Biochemistry, University of Pittsburgh School of Medicine, Pittsburgh, PA 15261. Phone: (412) 648-9947. Fax: (412) 624-1401.

ICP6, and the L/STs (OrfP) are efficiently expressed (4, 11, 34, 35, 79). Infection of cells with ICP4 mutants promotes the rapid destruction of most cells in culture (29), whereas UV-irradiated virus (29) and mutant viruses that are also deficient in the activation function of VP16 (30) are significantly less toxic. ICP4 mutants also cause chromosomal aberrations and rapid cell death (29). Johnson and colleagues have shown that either ICP4, ICP0, ICP27, or ICP22 can significantly reduce the transformation efficiency of cultured cells to G418 resistance (30). Therefore, a tenable hypothesis is that the activities of IE proteins perturb host cell metabolism, reducing cell viability.

We have been constructing viruses that have deletions of specific IE genes and sets of IE genes in an effort to uncover possible interactions between IE proteins and to understand how HSV initially alters host cell metabolism. In addition, current virus-based strategies for using HSV as a gene transfer vehicle have not met with success. For this purpose, it is desirable to gain an understanding of how HSV affects host cell metabolism in the absence of ICP4, as well as construct mutants in the genes that contribute to the observed deleterious effects. We have previously reported viruses that contain mutations in the essential IE genes, ICP4 and ICP27, and the complementing cell lines used for their isolation and propagation (59). This report describes the consequences of the additional inactivation of the ICP22 gene. In contrast to viruses deficient in ICP4 alone or ICP4 and ICP27, viruses deficient in ICP4, ICP27, and ICP22 minimally affect cell structure. Viral and cellular gene expression continues for at least 3 days. However, cellular DNA replication and cell division are inhibited. These findings have implications for how ICP0 might affect host cell metabolism and also indicate the need to eliminate ICP0 expression if HSV is to be effectively used as a replication-defective gene transfer vehicle.

MATERIALS AND METHODS

Cells and viruses. Vero cells and human embryonic lung (HEL) cells were propagated in Dulbecco's modified Eagle's medium (DMEM) containing 10% fetal bovine serum as described previously (76). The Vero-derived cell lines which provide HSV-1 IE functions in *trans*, E26 (ICP4 and ICP27), E5 (ICP4), and E8 (ICP27), were previously reported (11, 13, 59). All viruses are derived from wild-type HSV-1 strain KOS. The ICP27 and ICP22 double mutant, DMP, contains the 5*dl*1.2 (39) and *n*199 (55) mutations, respectively. The ICP4 and ICP27 double mutant *d*92 was previously described (59). *d*120 (ICP4$^-$) and 5*dl*1.2 (ICP27$^-$) were previously described (11, 39). Mutant viruses were propagated and titers were determined on the appropriate cell lines complementing the defective essential viral function for productive replication. Stocks of mutant virus were tested for the quantity of viral DNA reaching the nucleus following infection and also for the expression of ICP0 by immunofluorescence as a function of multiplicity of infection (MOI) to ascertain differences in the ratio of infectious virus to PFU. The results of these tests did not indicate a significant difference in this ratio with the different viruses.

DNA preparation and Southern blot analysis. Small-scale viral DNA preparations were obtained from 2×10^5 productively infected cells. Cells were harvested when cytopathic effects were generalized. After a cycle of freezing and thawing, the suspension was sonicated and pelleted in a microcentrifuge for 30 min at 4°C. The pellet was washed with Tris-buffered saline and lysed in digestion buffer containing 0.8% sodium dodecyl sulfate (SDS) and 400 μg of proteinase K per ml for 4 h at 37°C. After phenol-chloroform extraction, the DNA was precipitated by ethanol and resuspended in TE (10 mM Tris-HCl [pH 8.0], 1 mM EDTA).

For Southern blot analysis, viral DNA samples were digested with an appropriate restriction enzyme. Digested DNA samples were subjected to electrophoresis on a 0.7% agarose gel, stained with ethidium bromide, photographed, and transferred to a nitrocellulose membrane. Prehybridization, hybridization, and washing were performed according to standard protocols (60, 69). The membrane was exposed to Amersham Hyperfilm MP.

RNA preparation and Northern (RNA) blot analysis. RNA samples were prepared by infecting 1.5×10^6 cells in 60-mm-diameter culture dishes with viruses at an MOI of 10 PFU per cell. At the appropriate time postinfection, total RNA was isolated by using the Biotecx Ultraspec RNA isolation system (3a) as recommended by the manufacturer. The final RNA pellet was resuspended in diethylpyrocarbonate-treated water, and its concentration was determined by measuring the optical density at 260 nm.

For Northern blot analysis, 5 μg of RNA was denatured in denaturing buffer (65% formamide, 8% formaldehyde, 1 mM EDTA, 20 mM morpholinepropanesulfonic acid [MOPS], 8 mM sodium acetate) with ethidium bromide (0.5 μg/ml) at 68°C for 15 min. After being mixed with RNA loading buffer, the samples were subjected to electrophoresis on 1.3% formamide denaturing agarose gels at 35 V overnight with constant buffer circulation (28). Following electrophoresis, the gel was rinsed in water, and equal amounts of RNA samples were checked and recorded by photography on a UV transilluminator. The RNA was transferred to a nitrocellulose membrane in 20× SSC (3 M sodium chloride, 0.3 M trisodium citrate), air dried, and baked at 80°C for 2 h. Prehybridization and hybridization were performed as described previously (60). To detect HSV-1 ICP0, *tk* (thymidine kinase gene), and cellular β-tubulin mRNAs, ^{32}P-labeled nick-translated plasmid fragments from pW3dHS8 (58) digested with *Sac*I and *Pst*I, pTKSS (59) digested with *Eco*RI and *Bam*HI, and pRT3beta (5) digested with *Pst*I were used, respectively. Quantitation of Northern blots was performed with the AMBIS 4000 radioanalysis imaging detector system.

Electrophoresis of proteins. Viral and cellular protein expression was analyzed by SDS-polyacrylamide gel electrophoresis (PAGE) of virus-infected cells labeled with $^{32}P_i$ or [^{35}S]methionine. Vero or HEL cells (5×10^5) were seeded on 35-mm-diameter culture dishes. Viral infection was carried out in 0.1 ml of DMEM at an MOI of 10 PFU per cell at 37°C and 5% CO_2 with occasional rocking for 1 h. For [^{35}S]methionine labeling, 100 μCi of [^{35}S]methionine was added to methionine-deficient DMEM for 1 h at the indicated time. For $^{32}P_i$ labeling, 100 μCi of $^{32}P_i$ was added to phosphate-deficient DMEM at 2 to 6 h postinfection. After labeling, the cell monolayer was washed twice with Tris-buffered saline containing 500 μM *N-p*-tosyl-L-lysine chloromethyl ketone (TLCK). The infected cells were lysed in protein sample buffer (2% SDS, 50 mM Tris-HCl [pH 7.0], 5% β-mercaptoethanol, 0.005% bromophenol blue, 5% sucrose) and subjected to electrophoresis on an SDS–9% polyacrylamide gel. The gel was dried under vacuum and exposed to Amersham Hyperfilm.

DNA synthesis assay. To analyze DNA synthesis in cells, 1.5×10^6 cells seeded on 60-mm-diameter culture dishes were infected with virus at an MOI of 10 PFU per cell and then incubated for 1 h at 37°C and 5% CO_2 in 0.2 ml of medium. Following adsorption, the monolayers were washed twice and fresh medium was added. At the indicated time points, 100 μCi of [^{3}H]thymidine (New England Nuclear) was added for 3 h. After labeling, total DNA was isolated as described above except that the samples were also treated with RNase. Purified DNA was dissolved in TE, and its concentration was determined by measuring the optical density at 260 nm. The amount of ^{3}H incorporated was determined by liquid scintillation spectroscopy.

Colony-forming inhibition assays. Monolayers of 1.5×10^6 Vero cells were infected as described above with the indicated virus at the indicated MOI. An uninfected monolayer was maintained as a control. At 6 h postinfection, the monolayers were washed with Tris-buffered saline and trypsinized to generate single-cell suspensions. The suspensions were serially diluted and plated on 60-mm-diameter petri dishes in quadruplicate. For the efficient development of colonies, the fetal bovine serum concentration was raised to 20% and the medium was changed every 4 days. Approximately 2 weeks postplating, the colonies were fixed, stained with crystal violet, and counted. The fraction of surviving cells was represented relative to that obtained with uninfected monolayers.

Electron microscopy. Confluent monolayers of infected and uninfected cells were fixed in 2.5% glutaraldehyde in phosphate-buffered saline (PBS) for 1 h. Following fixation, the monolayers were postfixed with 1% osmium tetroxide containing 0.1% potassium ferricyanide, dehydrated through graded alcohol, and embedded with epoxy resin. Sections (50 to 60 nm) were cut with a Reichert Ultracut E ultramicrotome, mounted on 200-mesh grids, double stained with 2% uranyl acetate (7 min) and 1% lead citrate (3 min), and examined in a JEOL 100 CX electron microscope.

Immunofluorescence. Infected and uninfected cells were prepared on circular coverslips. Following incubation of the cultures, the culture medium was removed, and the cells were washed three times (5 min each) in PBS, fixed and permeabilized in −20°C methanol for 15 min, air dried, and then rehydrated in PBS. This procedure was followed by three washes (5 min each) in PBS containing 0.5% bovine serum albumin (BSA) and 0.15% glycine (BSA buffer). Nonspecific activity was blocked with 5% normal goat serum in BSA buffer. Subsequently, the sections were incubated for 2 h with a mouse monoclonal antibody against ICP0 (Goodwin Institute, Fla.) at a dilution of 1:100. Following incubation, the sections were washed three times in BSA buffer, and the primary antibody was revealed with a specific goat anti-mouse–Cy3.18 immunoconjugate (Jackson Laboratories). To image the DNA, cells were then washed for 2 min with Hoescht 33258 (2 μg/ml) and mounted in Gelvatol (Monsanto). Image fields were collected directly at the microscope, using a 60×, high-numerical aperture, color-corrected oil immersion objective; a high-sensitivity, integrating three-chip Sony color camera (700 by 600 pixels); and a Corecco frame grabber board in conjunction with a Nikon FXA photomicroscope. For fluorescent images, appropriate cubes, in perfect registration, were used to collect the ICP0 and DNA signals. A further differential interference contrast image was collected to assess cellular morphology at high resolution.

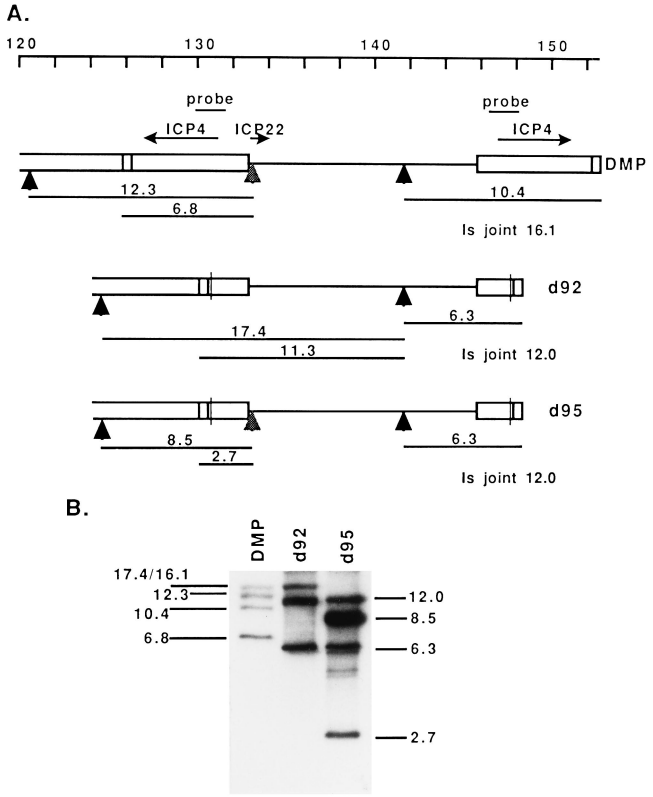

FIG. 1. (A) Schematic genome map from nucleotide 120 to the S terminus showing the locations of ICP4 and ICP22. The mutant virus, DMP, encodes a truncated ICP22 peptide of 199 amino acids by virtue of the insertion of a *Hpa*I linker encoding stop codons in all three reading frames (indicated by vertical arrowheads under the ICP22 gene). The remaining arrowheads mark the natural sites of *Hpa*I cleavage. Boxed regions represent the repeat region of HSV-1 viral genome. The lined region represents the unique short region of the HSV-1 genome. ICP22 and ICP4 (two copies) transcripts are represented by arrows. The *Hpa*I restriction fragments and their sizes (in kilobases) are represented under the maps of the viruses. (B) Southern blot analysis. DMP, *d*92, and *d*95 viral DNAs were digested by *Hpa*I and subjected to electrophoresis in a 0.7% agarose gel. The fractionated DNA fragments were transferred to a nitrocellulose membrane and probed with ^{32}P-labeled 1.84-kb *Bam*HI Y fragment (probe). The sizes (in kilobases) of the bands are marked.

RESULTS

An ICP4-, ICP27-, ICP22-deficient (*d*95) virus was generated by coinfecting E26 cells (59), which supply ICP4 and ICP27, with *d*92 (59) and the virus DMP. DMP is defective for ICP27 and ICP22 by virtue of the 5*dl*1.2 (39) and *n*199 (55) alleles, respectively. As previously described, *d*92 is defective for ICP4 and ICP27 by virtue of the *d*120 (11) and 5*dl*1.2 alleles (39), respectively. Therefore, both viruses used in this cross contain the 5*dl*1.2 allele, ensuring that the progeny will also contain this allele. The progeny from the coinfection were plaqued on E26 cells, and individual plaques were isolated and screened for the ability to grow on ICP4- and ICP27-expressing E26 cells and not on E8 cells, which supply only ICP27. This manipulation was performed to restrict the further analysis of progeny to isolates that were genetically deficient in ICP4. Isolates that grew only on E26 cells were then screened for the incorporation of the *n*199 allele by Southern blot hybridization. *n*199 is marked by an *Hpa*I site, which is part of a linker that specifies the stop codon conferring the ICP22$^-$ phenotype.

Figure 1A shows the genome of HSV from nucleotide 120 to the S terminus in the parental orientation, the locations of the genes for ICP4 and ICP22, and the structures of DMP, *d*92, and *d*95 relative to the relevant *Hpa*I restriction sites (vertical arrowheads). Also shown are the expected sizes of the *Hpa*I fragments that span the ICP4 gene. The expected size of the Is joint fragment is listed for clarity. Figure 1B shows a Southern blot of the *Hpa*I restriction digests of *d*92, DMP, and *d*95 probed with the *Bam*HI Y fragment (Fig. 1A), demonstrating the incorporation of the *n*199 insertion into the *d*95 background. The sizes of the shortened fragments in the digest of *d*95 relative to *d*92 are consistent with the incorporation of the *n*199 allele into *d*95. The sizes of the shortened fragments in the digest of *d*95 relative to DMP are consistent with the incorporation of both of the 4.1-kb deletions of the ICP4 coding sequence in *d*92 into *d*95. Therefore, the *Hpa*I pattern of this region of *d*95 is consistent with the presence of mutations in both copies of the ICP4 gene and in the ICP22 gene. The plaquing behavior of *d*95 on E26, E5, and E8 cells is consistent with the presence of mutations in both copies of the ICP4 gene and the ICP27 gene.

To visualize the IE proteins synthesized in mutant-infected cells and verify the lack of ICP4, ICP27, and ICP22 synthesis, cycloheximide-treated Vero cell monolayers were infected with the indicated viruses at an MOI of 10 PFU per cell and incubated in the presence of cycloheximide for 6 h. The cycloheximide was then removed by washing the monolayer, and incubation was continued in the presence of actinomycin D and [^{35}S]methionine. Under these conditions, only the IE proteins are labeled (10, 26). While ICP4, ICP0, ICP27, and ICP22 were visible in the profiles of KOS-infected cells, the individual mutants were missing the bands corresponding to the intended mutations in the IE genes (Fig. 2A). Thus, *d*95 does not synthesize ICP4, ICP27, or ICP22. The proteins synthesized in cells infected with *d*120, 5*dl*1.2, and *d*92 are consistent with the previously reported genotypes and phenotypes of these viruses (11, 39, 59). Also included on this gel is a sample of *d*96-infected cells. *d*96 was generated by a backcross of *d*95 with wild-type virus and screening for progeny that grow on E5 cells and not on Vero cells. *d*96 does not synthesize ICP4 or ICP22.

To further demonstrate that *d*95 does not synthesize ICP4, ICP27, or ICP22, cells infected with *d*120 (ICP4$^-$), *d*92 (ICP4$^-$ ICP27$^-$), and *d*95 (ICP4$^-$ ICP27$^-$ ICP22$^-$) were metabolically labeled with $^{32}P_i$, and extracts of these cells were analyzed by SDS-PAGE. ICP27 and ICP22 are readily labeled with ^{32}P, making this approach a very good one to visualize these proteins. The resulting autoradiogram is shown in Fig. 2B. The band corresponding to ICP27 was missing in both *d*95 and *d*92, while that corresponding to ICP22 was missing in *d*95. The lack of ICP22 in *d*95 was also evident in the [^{35}S]methionine profile in Fig. 4. None of the mutants in Fig. 2 synthesized ICP4.

Prolonged viral and cellular gene expression in *d*95-infected cells. Levels of viral and cellular gene expression were compared in *d*92- and *d*95-infected Vero cells by SDS-PAGE analysis and Northern blot analysis. One effect that became evident early in the course of this study was that cells infected with *d*120, *d*96, and *d*92 at an MOI of 10 PFU per cell could be analyzed only up to 1 day postinfection, whereas cells infected with *d*95 retained a morphology more closely resembling, but not identical to, that of uninfected cells (Fig. 3). While the *d*120- and *d*92-infected cell monolayers were virtually destroyed at 2 days postinfection, the *d*95 monolayer was intact (Fig. 3A). It is also interesting that there were fewer *d*95-infected than uninfected cells at this time and that many of the *d*95-infected cells consisted of two nuclei in one cytoplasmic boundary. The same general effects on toxicity and cell number were observed on HEL cells (Fig. 3B), although it was difficult to observe multinucleated cells at this level of resolution. As a

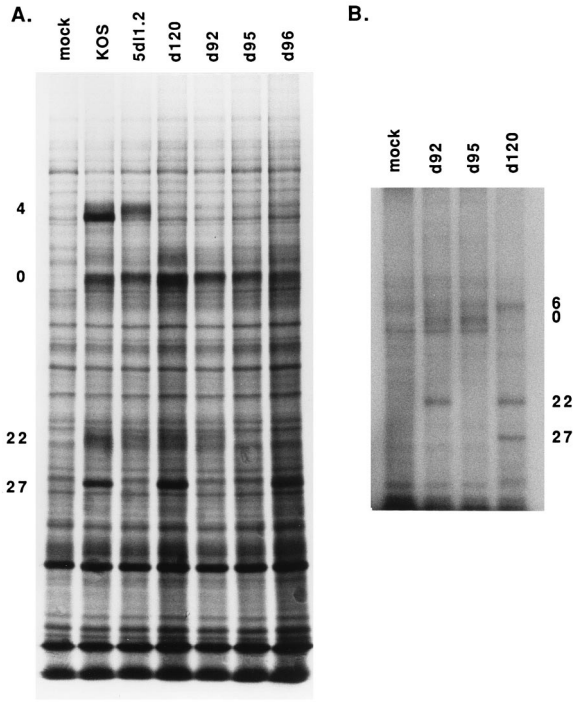

FIG. 2. IE proteins specified by wild-type and mutant viruses. (A) Cycloheximide reversal experiment. Vero cell monolayers were pretreated for 1 h by incubation in cycloheximide (100 μg/ml)-containing medium, infected with KOS (wild type), 5*dl*1.2 (ICP27$^-$), *d*120 (ICP4$^-$), *d*92 (ICP4$^-$ ICP27$^-$), *d*95 (ICP4$^-$ ICP27$^-$ ICP22$^-$), and *d*96 (ICP4$^-$ ICP22$^-$) at an MOI of 10 PFU per cell, and incubated in the presence of cycloheximide for 6 h. The monolayers were then washed twice and further incubated for 3 h in presence of actinomycin D (10 μg/ml) and [^{35}S]methionine (100 μCi per plate). The cells were lysed in SDS sample buffer and subjected to electrophoresis on an SDS–9% polyacrylamide gel. The viral proteins ICP4, ICP0, ICP22, and ICP27 are indicated on the left. (B) Phosphoprotein synthesis in *d*95-, *d*120-, and *d*92-infected cells. Monolayers of Vero cells on 35-mm-diameter petri dishes were infected with *d*92, *d*95, and *d*120 at an MOI of 10 PFU per cell. At 2 h postinfection, the medium was replaced with phosphate-deficient medium containing 100 μCi of $^{32}P_i$. Cell extracts were lysed and analyzed on an SDS–9% polyacrylamide gel. ICP6, ICP0, ICP22, and ICP27 are marked on the right.

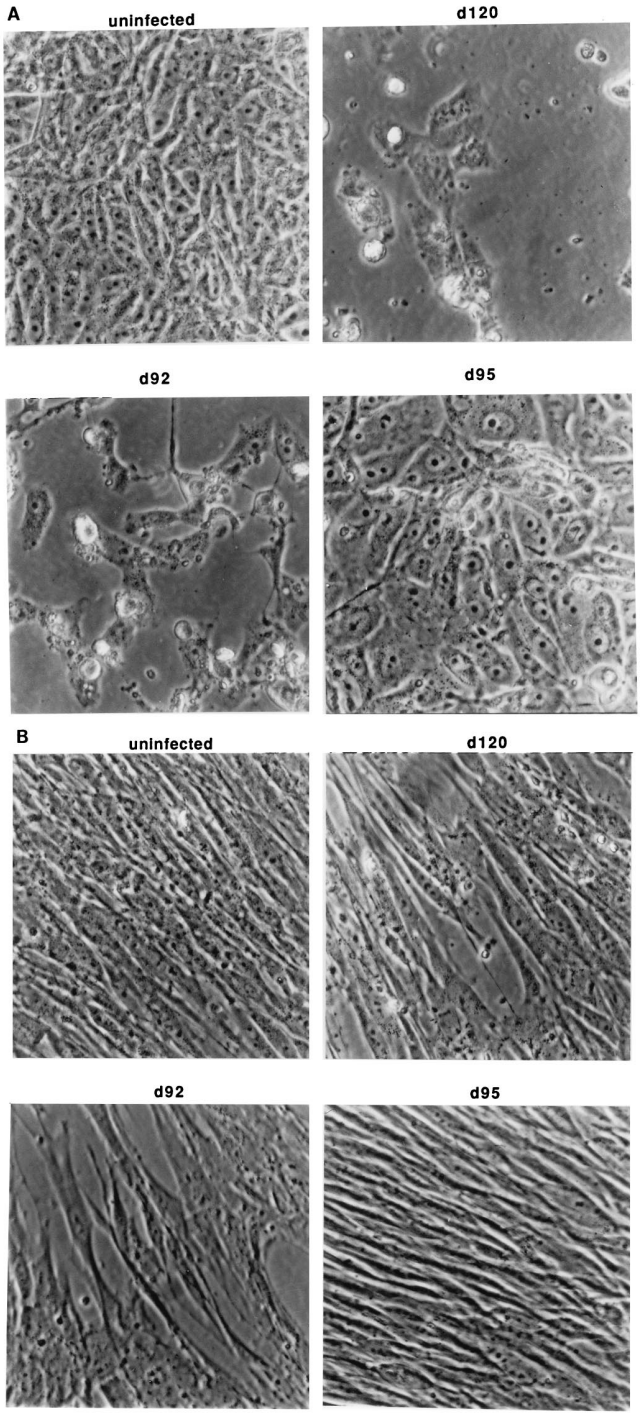

FIG. 3. Apparent cytotoxicity of *d*95, *d*120, and *d*92. (A) Toxicity to Vero cells. Confluent monolayer of 5×10^5 Vero cells were infected with *d*120, *d*92, and *d*95 at an MOI of 10 PFU per cell and incubated for 2 days. The culture were photographed through a 40× phase-contrast objective. (B) Toxicity to HEL cells. The assay was performed as described above except that 10^6 HEL cells were used per monolayer.

consequence of the cytotoxicity of *d*120, *d*92, and *d*96, it was only possible to analyze viral and cellular gene expression in *d*95-infected cells past 1 day postinfection.

*d*92- and *d*95-infected Vero cells were analyzed for viral and cellular protein synthesis. Monolayers of Vero cells were infected at an MOI of 10 PFU per cell and labeled for 1 h with [^{35}S]methionine at the indicated times postinfection, and cell extracts were subjected to SDS-PAGE analysis. The resulting SDS-PAGE profile is shown in Fig. 4. Several observations can be made from these results. (i) The ICP22 band was clearly evident in the 6-, 12-, and 24-h *d*92 samples and not in the corresponding *d*95 samples. (ii) There was very little *d*92 sample at 2 and 3 days postinfection. This was due to loss of cells at this time and is consistent with the results shown in Fig. 3. (iii) Cellular protein synthesis in *d*95-infected cells remained quite high even at 3 days postinfection. This is evident by comparison with the mock-infected sample. (iv) The viral proteins ICP0 and ICP6 were abundantly expressed even at 3 days postinfection. *d*120 and *d*96 behaved like *d*92 with respect to the lack of longevity of protein synthesis (data not shown). This is presumably due to the toxic effects of these viruses and is consistent with the results of Johnson and colleagues (29).

To further assess gene expression in *d*95-infected cells, the abundances of several RNA species were determined. Figure 5A shows levels of ICP0, *tk*, and cellular β-tubulin RNAs in *d*120-, *d*92-, and *d*95-infected cells and in uninfected cells at 6 and 24 h postinfection. Also shown is an experiment in which the levels of these transcripts were determined in uninfected

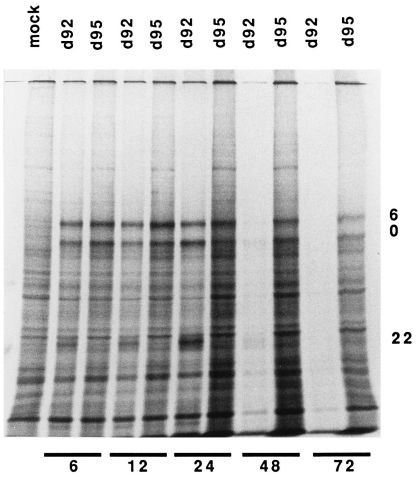

FIG. 4. Viral and cellular protein synthesis in *d*92- and *d*95-infected cells. Vero cells (5×10^5) seeded on a 35-mm-diameter petri dish were infected with *d*92 and *d*95 at an MOI of 10 PFU per cell. At 6, 12, 24, 48, and 72 h postinfection, cells were pulse-labeled for 1 h by incubation in presence of 100 μCi of ^{35}S-labeled methionine per ml. After the labeling period, the cells were solubilized in SDS sample buffer and electrophoresed on an SDS–9% polyacrylamide gel. The positions of ICP0, ICP6, and ICP22 are indicated on the right.

and *d*95-infected cells at 24, 48, and 72 h postinfection (Fig. 5B). It should be noted that while ICP0 is abundantly transcribed in the absence of ICP4, *tk* is not. The levels of *tk* seen in the absence of ICP4 are approximately 2 to 4% of those seen in the presence of ICP4 (28). Consistent with previous studies, ICP0 RNA was slightly increased in size in *d*92-infected cells relative to *d*120-infected cells, and the abundance of *tk* RNA was less in *d*92-infected cells than in *d*120-infected cells, at 6 h postinfection (59). Curiously, deletion of ICP22 from the *d*92 background suppressed these effects. The effect on ICP0 RNA was less evident at 24 h postinfection, and the effect on *tk* RNA was no longer observed. Consistent with the labeling of cellular

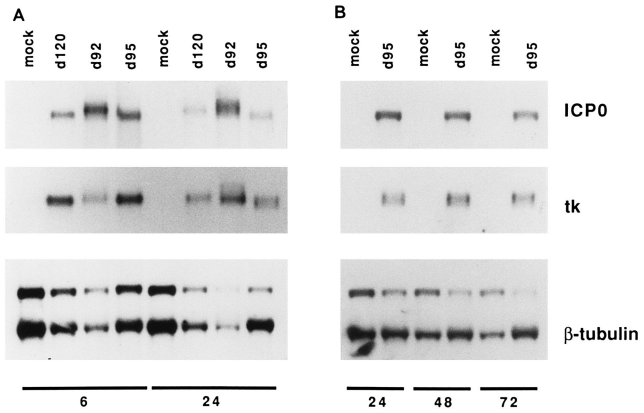

FIG. 5. Accumulation of ICP0, *tk*, and β-tubulin RNAs in *d*120-, *d*92-, and *d*95-infected Vero cells. Vero cells were mock infected or infected with *d*120, *d*92, and *d*95 at an MOI of 10 PFU per cell. At 6 and 24 h postinfection, total RNA was isolated and 5 μg of each sample was subjected to Northern blot analysis. ICP0, *tk*, and β-tubulin RNAs were probed with the probes described in Materials and Methods (A). Uninfected and *d*95-infected Vero cells (MOI of 10) incubated for 1, 2, and 3 days were analyzed in a similar manner (B). Because of alternative polyadenylation site usage, two β-tubulin mRNAs were detected. The 1.8-kb species results from utilization of the proximal poly(A) site, and the 2.6-kb species results from utilization of the distal poly(A) site.

proteins in the SDS-PAGE profile in Fig. 4, the abundance of β-tubulin RNA was greatest in the *d*95-infected cells, being comparable to that in uninfected cells. Therefore, despite the equal loading of total cellular RNA as determined spectrophotometrically and by the ethidium bromide staining patterns of the rRNA, β-tubulin RNA was less abundant in *d*120- and *d*92-infected cells than in *d*95-infected cells. This finding implies that the stability or the transcription of these messages is reduced as a consequence of the genes expressed in *d*120 and *d*92 and that the further removal of ICP22 relieved this effect. The abundances of all three of the messages in *d*95-infected cells remained relatively unchanged up to 3 days postinfection (Fig. 5B). However, after 3 to 4 days at an MOI of 10, the monolayer lost its integrity; consequently, these times were not analyzed. The same patterns of expression of ICP0, *tk*, and β-tubulin RNAs seen in Vero cells were also seen in HEL cells (data not shown).

Quantitative analysis of the β-tubulin RNA in Fig. 5 is shown in Fig. 6. At 6 and 24 h postinfection, the levels of β-tubulin RNA were reduced in *d*120-, *d*92-, and *d*95-infected cells, with the least reduction seen in *d*95-infected cells (Fig. 6A). While the levels of β-tubulin RNA declined in uninfected cells over the course of 3 days, β-tubulin RNA levels in *d*95-infected cells remained constant over this time period (Fig. 6B), as did the levels of ICP0 and *tk* RNAs over this time interval (Fig. 5B). The simplest interpretation of the data is that HSV proteins expressed from the *d*95 genome, including ICP0, allow for transcription to continue at a constant rate over the 3-day period.

It is clear from Fig. 5 that β-tubulin RNA is present in two species. This has been previously reported and results from the use of alternative polyadenylation signals (36). Figures 6C and D show the ratios of the low (1.8-kb)- to high (2.6-kb)-molecular-size species, indicative of the relative usage of the proximal and distal poly(A) sites. This usage changed as a function of the viral genetic background by 1 day postinfection. Utilization of the proximal signal increased when ICP27 was deleted, as demonstrated by the increase in the low/high ratio in *d*92- and *d*95-infected cells relative to *d*120- and mock-infected cells at 24 h postinfection (Fig. 6C). The usage of the proximal poly(A) site became more pronounced by 2 and 3 days postinfection in *d*95-infected cells relative to uninfected cells (Fig. 6D). Therefore, the HSV proteins expressed from the *d*95 genome, including ICP0, result in the alteration of 3′ processing relative to uninfected cells in the case of β-tubulin RNA. It is also possible that the *d*95 background results in an altered relative stability of the two processed forms of the message. Apparently, the added expression of ICP27 results in the alteration of poly(A) site usage back to a proportion observed in uninfected cells.

Inhibition of cell division and DNA replication in *d*95-infected cells. While cells infected with *d*95 do not exhibit rapid rounding up and detachment from the monolayer and continue to express viral genes for at least 3 days, they do not increase in number. This is evident to some degree in Fig. 3 and is represented quantitatively in Fig. 7A. While uninfected Vero cells in a monolayer increased in number over 2 days, *d*95-infected cells did not. Rather, a marginal decrease in cell number was evident. Therefore, it appears the growth potential of *d*95-infected cells was inhibited.

To assess the growth potential of *d*95-infected cells, two experiments were performed. The first involved infecting monolayers of Vero cells with *d*120, *d*92, and *d*95 at several multiplicities, followed by trypsinization and plating to measure CFU (Fig. 7B). The second measured incorporation of [^{3}H]thymidine into infected cell DNA (Fig. 7C and D). In the

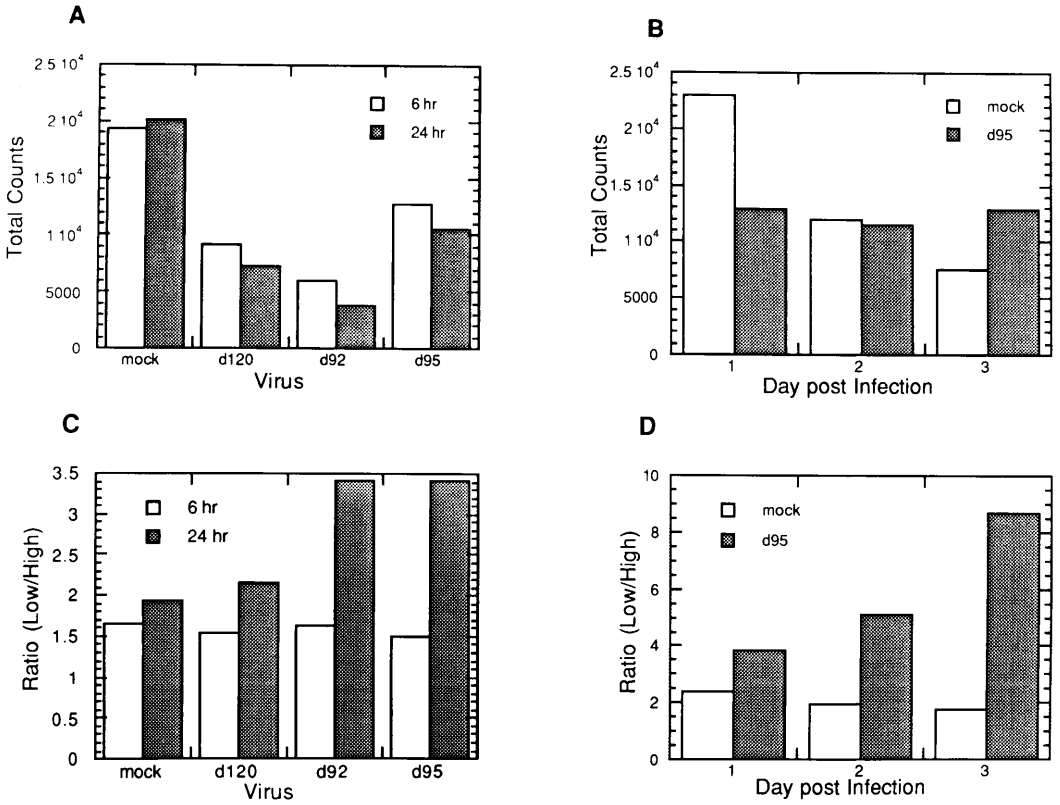

FIG. 6. Quantitation of mRNA accumulation and poly(A) site usage of cellular β-tubulin. (A) Counts of ^{32}P hybridizing to the 1.8- and 2.6-kb species in Fig. 5A were determined as described in Materials and Methods. (B) Counts of ^{32}P hybridizing to the 1.8- and 2.6-kb species in Fig. 5B were determined as described in Materials and Methods. (C) The ratios of the net counts of the 1.8-kb over 2.6-kb species in Fig. 5A. (D) The ratios of the net counts of the 1.8-kb over 2.6-kb species in Fig. 5B.

colony-forming assay, *d*92 inhibited cell viability less than *d*120. Interestingly, *d*95 was only marginally less inhibitory than *d*92, despite the dramatically different appearance of *d*92- and *d*95-infected cells shown in Fig. 3. Figure 7B also shows the probability of the cells not being infected following inoculation at a given MOI. The survival curves indicate that up to an MOI of 3, a single PFU is very efficient in inhibiting colony formation. At an MOI of 10, survival is greater than would be expected from the pattern seen at the lower MOIs. This finding indicates that the inhibitory effects may be saturable or that there may be subpopulations of cells that are less susceptible to the inhibitory effects of IE proteins. In summary, all of these viruses had a significant inhibitory effect on colony-forming ability, indicating that fundamental cellular processes required for cells to form colonies are perturbed by HSV, even when ICP4, ICP27, and ICP22 are not expressed.

To study this effect in greater detail, we determined if cellular DNA synthesis was inhibited in *d*95-infected cells. Accordingly, Vero and HEL cells were infected with *d*95 at an MOI of 10 PFU per cell. At 1, 2, 3, and 4 days postinfection, *d*95-infected and uninfected cells were labeled for 3 h with [^{3}H]thymidine. Following the labeling period, DNA from the cells was isolated and the amount of ^{3}H incorporated per microgram of DNA was determined. As is evident in Fig. 7C and D, *d*95 infection significantly inhibited cellular DNA replication in both Vero and HEL cells, respectively. The reduction in labeling of uninfected cells at 3 and 4 days postinfection is consistent with results of Fig. 7A, probably reflecting contact inhibition. To determine the level of DNA synthesis as a function of the other IE mutant backgrounds, Vero cells were infected with *d*120, *d*92, *d*95, and *d*96 at an MOI of 10 PFU per cell and labeled with [^{3}H]thymidine from 21 to 24 h postinfection. As described above, DNA was isolated and the quantity of ^{3}H incorporated per microgram of DNA was determined. The resulting levels of incorporation of [^{3}H]thymidine relative to that in uninfected cells were 25% for *d*120, 12% for *d*92, 13% for *d*95, and 25% for *d*96. These results suggest that the cellular environment in all of these mutant backgrounds is incompatible with uninfected levels of cellular DNA synthesis.

Perturbation of nuclear structure by HSV IE gene mutants. It has been known for some time that ICP4 mutants of HSV have a deleterious effect on cellular morphology and chromatin structure (29, 49). To determine the contributions of the IE proteins to morphological changes in the cell, Vero cells were infected at an MOI of 10 PFU per cell with *d*120, *d*92, *d*95, and *d*96 and processed for electron microscopy at 24 h postinfection. Figure 8 shows that all of the mutants elicit changes or the formation of novel structures relative to uninfected cells. Normal cell morphology is shown in Fig. 8A. Infection of cells with *d*120 (Fig. 8B) resulted in the accumulation of small dense intranuclear granules. The nucleus commonly had a highly convoluted profile, and frequently a series of large proteinaceous cytoplasmic bodies was seen. *d*96 (Fig. 8F) had morphologic sequelae similar to those for d120 except that the small dense intranuclear granules were absent. In *d*92-infected cells (Fig. 8C), no large cytoplasmic bodies were seen; rather, these structures were confined to the nucleus. The *d*92-infected cells also showed small nuclear granules (as seen in the *d*120-

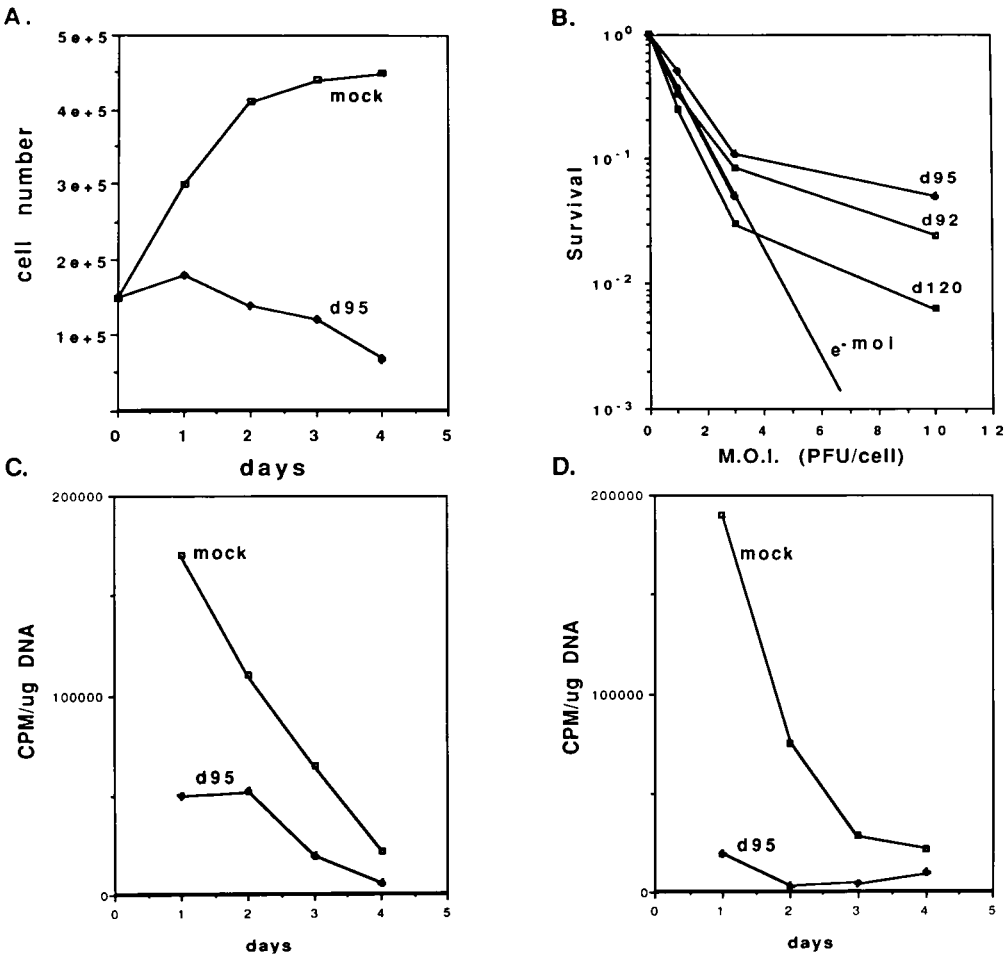

FIG. 7. Growth potential of *d*95-infected cells. (A) Cell number as a function of time postinfection with *d*95. Monolayers of Vero cells were mock infected or infected with *d*95 at an MOI of 10 PFU per cell. At 1, 2, 3, and 4 days postinfection, the monolayers were trypsinized and the cells were counted in a hemocytometer. Shown are the cell counts per milliliter from a 3-ml suspension. (B) Colony inhibition assay. Confluent monolayers of Vero cells were mock infected or infected with the indicated viruses and MOIs. The monolayers were trypsinized at 6 h postinfection and plated for CFU as described in Materials and Methods. Shown are the surviving fraction of infected cells relative to uninfected cells. Also shown is the probability of a cell not becoming infected as a function of MOI (e^{-moi}). (C) Incorporation of [^{3}H]thymidine into Vero cell DNA as a function of time after infection with *d*95. Monolayers of Vero cells were mock infected or infected with *d*95 at an MOI of 10 PFU per cell. At 1, 2, 3, and 4 days postinfection, the cultures were labeled for 3 h with [^{3}H]thymidine, and the cellular DNA was extracted, quantified, and counted for ^{3}H as described in Materials and Methods. (D) Incorporation of [^{3}H]thymidine into HEL cell DNA as a function of time after infection with *d*95. This experiment was performed like that in panel C except that HEL cells were used in place of Vero cells.

infected cells); however, they commonly appeared as larger condensed structures about the large nuclear bodies (Fig. 8C and D). *d*95-infected cells appeared to be the least affected; however, numerous large and regularly shaped nuclear inclusions were evident in these cells (Fig. 8E). These inclusions were noticeably absent from uninfected cells and are reminiscent of the nuclear bodies seen in *d*92-infected cells.

ICP0 is abundantly synthesized in *d*95-infected cells (Fig. 4). To address the possibility that ICP0 is present in the dense nuclear bodies in *d*95-infected cells, *d*95-infected cells were stained with ICP0 antibody and processed for immunofluorescence microscopy. Shown in Fig. 9 are fluorescent images of *d*95-infected cells (MOI of 10 PFU per cell) stained with a monoclonal antibody to ICP0 at 6, 12, 24, and 48 h postinfection. The insets show an enlargement of a nucleus from the larger field. As previously observed (31, 81, 82), ICP0 accumulated in fine punctate structures at early times (6 h) postinfection (Fig. 8A). Subsequently, the continued accumulation of ICP0 in the nucleus resulted in the formation of fewer but much larger ICP0-containing bodies (Fig. 8B to D). The perturbation of nuclear structure and number often seen with IE mutants is evident in Fig. 8D and E. Figure 8E shows the same field as in Fig. 8D, but the DNA has been specifically stained with Hoescht dye. From this micrograph, it is clear that the ICP0-containing structures do not contain DNA. Figure 8F is a differential interference image of the same cell as in Fig. 8D and E. The ICP0-containing structures are easily resolved in this image. Thus, in the absence of ICP4, ICP27, and ICP22, ICP0 accumulated to very high levels in the nucleus and localized to dense, spherical bodies. The formation of these structures represents the only obvious deviation from the morphology of uninfected cell nuclei.

DISCUSSION

The ability of virus-encoded functions to rapidly usurp host cell metabolic mechanisms along with the function of viral systems enables HSV to express its 75 to 80 genes, replicate its genome, and assemble progeny within 6 h of infection in susceptible cells. While significant progress has been made toward

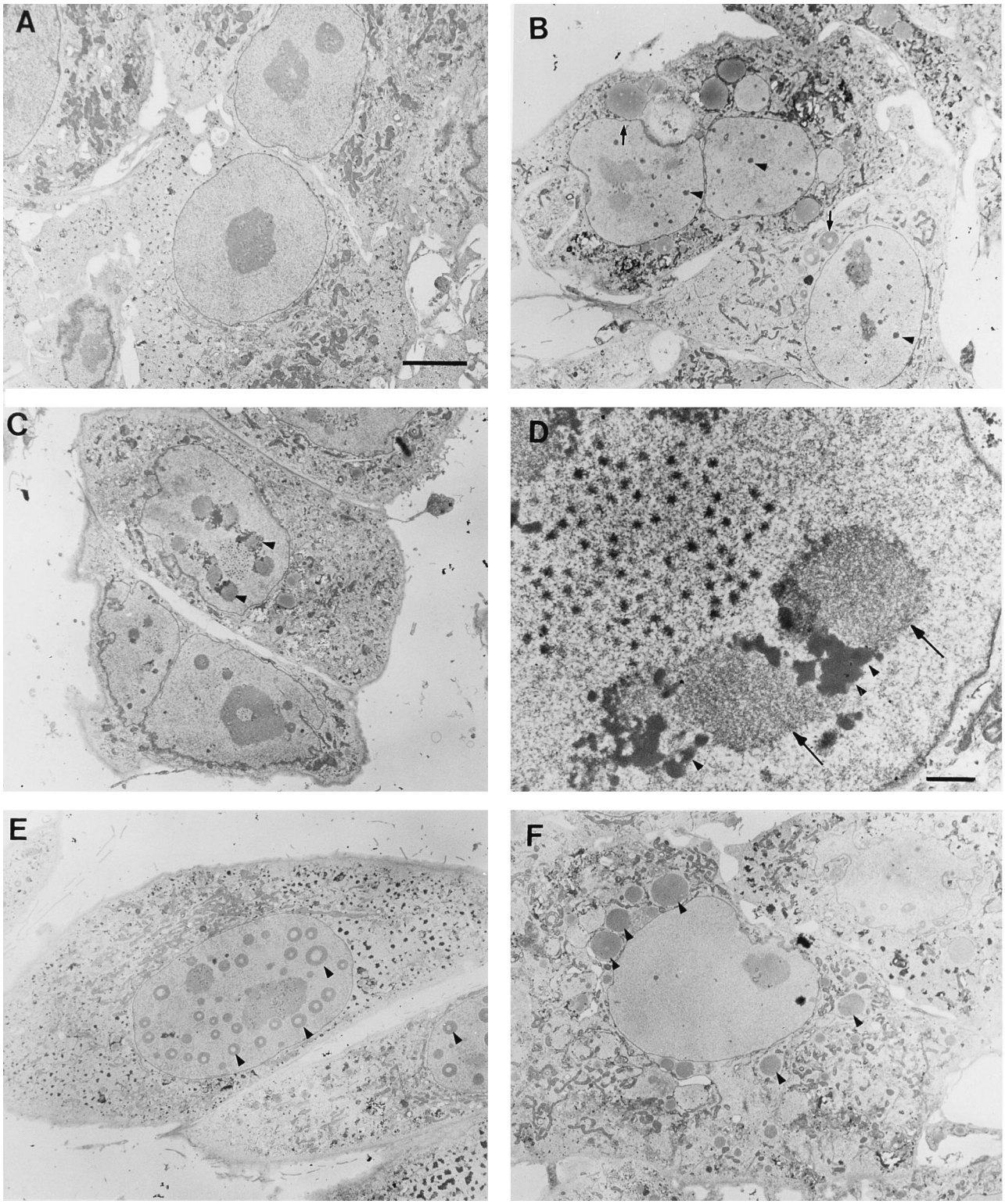

FIG. 8. Electron micrographs of Vero cells after infection with different IE mutants. Eighty percent confluent monolayers of Vero cells were uninfected or infected with *d*120, *d*92, *d*96, or *d*95 at an MOI of 10 PFU/ml. At 24 h postinfection, the monolayers were processed for electron microscopy as described in Materials and Methods. (A) Uninfected cells show a typical cell and nuclear morphology, with large prominent nucleoli and thin heterochromatin (bar = 5 μm). (B) Cells infected with *d*120. Small intranuclear (arrowheads) and large cytoplasmic (arrows) inclusions are apparent. Magnification as in panel A. (C and D) In cells infected with *d*92, at low power (C), large (arrowheads) and small intranuclear particles are apparent. At high power (D), the small particles are seen to exist both as small stellate granules and as structures condensed about the larger inclusions (arrows). C, magnification as in panel A; D, bar = 0.5 μm. (E) Cells infected with *d*95. Large abundant nuclear inclusions are seen (arrowheads). Serial sectioning shows these structures to be spherical (not shown). Magnification as in panel A. (F) Cells infected with *d*96. The nucleus appears similar to that seen in control cells (A); however, abundant, large cytoplasmic inclusions are apparent (arrowheads). Magnification as in panel A.

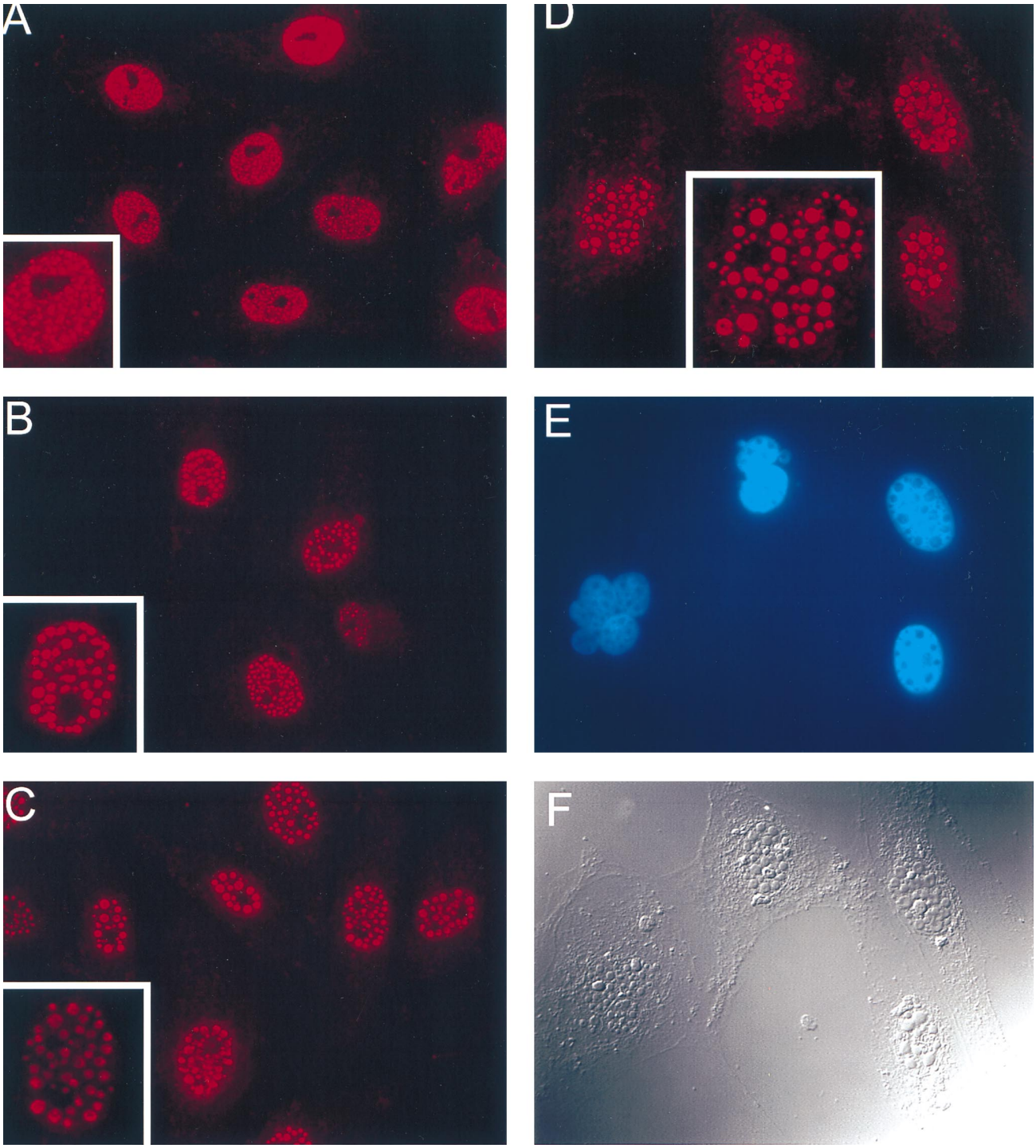

FIG. 9. Localization of ICP0 in *d*95-infected cells. Eighty percent confluent monolayers of Vero cells were infected with *d*95 at an MOI of 10 PFU/ml and processed for immunofluorescence at 6 (A), 12 (B), 24 (C), and 48 (D to F) h postinfection, using a monoclonal antibody to ICP0 as described in Materials and Methods. At early time points, the ICP0-containing nuclear inclusions appear small and granular, with a high nucleoplasmic staining. With time, the size of the inclusions increases dramatically, while the nucleoplasmic background staining decreases. (E) When the DNA within the nucleus is counterstained with Hoescht dye, it is apparent that the ICP0-staining granules contain no DNA. (F) When the cells are examined by differential interference contrast microscopy, while the cellular cytoplasmic profile appears normal, the multiple nuclear inclusions are apparent. Panels D to F are the same field.

the understanding of viral functions, less light has been shed on how these functions perturb or alter host cell processes.

It has been known for some time that infection of cells with viruses deficient in ICP4 results in rapid cell death (29) accompanied by chromosomal damage (29, 49) and alterations in nuclear structures. In the absence of ICP4, at least five other gene products, ICP27, ICP0, ICP22, ICP47, ICP6, and OrfP, are efficiently synthesized (4, 11, 34, 35, 79). Many of these

proteins have been shown to have activities that may perturb host cell functions. Indeed, it has been demonstrated that ICP27, ICP0, and ICP22 reduce the efficiency with which cells are transformed with a selectable marker, implying that they reduce cell viability (30).

In this study, the effects of a series of HSV mutants defective in ICP4, ICP22, and ICP27 on gene expression, host cell viability, cellular DNA replication, cell division, and nuclear ultrastructure were studied. These experiments revealed that infection of cells with a mutant defective in ICP4, ICP22, and ICP27 (*d*95) resulted in prolonged cell viability, as measured by viral and cellular gene expression (Fig. 4 and 5) and overall cell morphology relative to *d*120- and *d*92-infected cells. The colony-forming capacity, or the capacity of *d*95-infected cells to multiply, was not significantly greater than that of *d*92-infected cells (Fig. 7B), despite the large difference observed in the appearance of *d*92- and *d*95-infected monolayers (Fig. 3). Additionally, *d*95 had the least effect on nuclear morphology of all of the mutants tested (Fig. 8). The only deviation from uninfected cell morphology was the accumulation of dense, spherical structures in the nucleus, which were subsequently shown to contain ICP0 (Fig. 9).

Gene expression in mutant virus-infected cells. In HSV-1-infected cells, the transcription of viral and cellular genes is carried out by host RNA polymerase II (1). ICP4 has a direct effect on transcription, and ICP0, ICP27, and ICP22 have all been implicated in modulating transcription. ICP0 is a promiscuous transactivator which has been reported to transactivate a variety of viral and cellular promoters (16, 18, 47, 53). ICP0 is abundantly expressed in *d*95-infected Vero cells. The level of ICP0 transcript and the rate of ICP0 protein synthesis were relatively constant from days 1 to 3 postinfection. In addition, the accumulation of a cellular message was maintained at a high level throughout this time period. It is possible that the expression of ICP0 in the absence of the deleterious effects of other IE genes allows for the observed prolonged gene expression.

The striking difference in cell morphology and survival was observed when ICP22 was inactivated. Mutants in ICP22 show reduced transcription and expression of certain viral genes (55, 65). ICP22 also induces a novel phosphorylated form of cellular RNA polymerase II (55). These observations are all consistent with transcriptional effects, with the presence of ICP22 correlating with more efficient viral transcription. By virtue of the prolonged accumulation of the products of viral and cellular genes, we apparently see more efficient gene expression in the absence of ICP22. Previous studies of ICP22, including some using the same ICP22 allele in *d*95, have all focused on the effect of ICP22 in an otherwise wild-type background. It is possible that the prolonged gene expression that is observed in this study with *d*95 compared with *d*92 is related not to a direct effect of ICP22 on gene expression but rather to some other deleterious effect that is relieved by the inactivation of ICP22. Comparison of the activities of the transcriptional apparatus in *d*92- and *d*95-infected cells should shed some light on this question.

ICP27 has been shown to affect two aspects of mRNA processing: splicing and poly(A) site usage (23, 42, 43, 61–63). Effects on mRNA structure were observed in two cases in this study. The first is that the *tk* and ICP0 messages were slightly larger and appeared more heterogeneous when synthesized in the *d*92 (ICP4$^-$ ICP27$^-$) background compared with the *d*120 (ICP4$^-$) background. This effect was suppressed when ICP22 was mutated (*d*95). The second is that the deletion of ICP27 from the *d*120 background resulted in a change in the relative utilization of the β-tubulin poly(A) sites (Fig. 5 and 6) at 24 h postinfection. The further deletion of ICP22 had little or no effect on poly(A) site utilization; however, the effect became more pronounced because of the extended life span of the infected cells. This observation also demonstrates that in the *d*95 background, the poly(A) site usage may be different from that in uninfected cells. This effect is unexpected since none of the proteins expressed in this background is known to have an effect on poly(A) site usage. These observations on viral and cellular messages, the former in particular, are consistent with effects of ICP27 on poly(A) site selection (42, 43). The effect on ICP0 and *tk* messages also suggests a functional interaction between ICP27 and ICP22. Deleting ICP27 (in *d*92) resulted in altered mRNA structure relative to *d*120, and the further inactivation of ICP22 in *d*95 suppressed this effect.

Cytotoxicity and the inhibition of DNA synthesis. In the absence of ICP4, ICP27, and ICP22, the infected cell survives longer than cells infected with an ICP4$^-$ ICP27$^-$ mutant, as is clear from microscopic examination of cells and studies on cell and viral gene expression. Despite this, the ability of *d*95-infected cells to proliferate and form colonies was impaired. This impairment is due at least in part to factors contributing to the inhibition of cell DNA synthesis. Presumably, the proteins synthesized in the *d*95 background (ICP6, ICP0, ICP47, and OrfP) are responsible for this effect. ICP47, a cytoplasmic protein that has been shown to affect the processing of major histocompatibility complex class I molecules (80), is probably not responsible for this effect. ICP6 is also probably not involved since a virus deleted for ICP6, ICP4, and ICP27 still inhibits cell DNA synthesis (unpublished data). This leaves OrfP and ICP0 as potential candidates for this effect. Additionally, ICP0 may induce changes in cellular gene expression that result in the inhibition of cellular DNA synthesis or cell cycle arrest. It is also possible that the virion-associated host cell shutoff function, UL41 (53a), also contributes to the shutoff of host cell DNA synthesis. However, two observations suggest that this is at most a minor component of the shutoff of DNA synthesis: (i) at the MOIs used in this study, *d*95 did not efficiently shut off host cell protein synthesis (Fig. 3), and (ii) a virus lacking ICP4, ICP27, and UL41 still shuts off host cell DNA synthesis (data not shown).

ICP0 clearly alters the nuclear ultrastructure and potentially the compartmentalization of nuclear proteins involved in cell cycle regulation. In cells infected with wild-type virus (31) or an ICP4$^-$ ICP27$^-$ mutant (*d*92 [82]), ICP0 accumulates in many small punctate intranuclear structures. Everett and Maul have shown that these structures are coincident with PML-containing structures (17, 38), also known as ND10, PODs, or Kr bodies (2, 15, 32, 75, 78). The function of these structures is unknown but is thought to be involved in the proliferative or differentiation state of the cell (15, 32, 75). In a wild-type virus background, ICP0 dissociates these structures late in infection and itself becomes more diffusely localized throughout the cell (17, 38). In *d*95-infected cells, ICP0 accumulates over the course of 3 days (Fig. 3). Early in infection, its localization is similar to that seen previously, i.e., an abundance of small punctate structures is evident over a diffuse background. However, with time, ICP0 accumulates into increasingly large structures, which are clearly visible by light microscopy. These structures do not contain significant quantities of DNA. One possibility is that they represent inclusion bodies which have nucleated at the ND10 structures. From previous results, it is likely that ND10 structures are disturbed, and it is also possible that cellular molecules, which interact with ICP0, are sequestered into these inclusion bodies. Further studies on the compositions of these structures and the cellular proteins that they may contain are in progress. A remaining formal possibility is

that a truncated ICP22 molecule is synthesized as a function of *n*199 allele, and this peptide is involved in the phenotype of *d*95. However, the *n*199 allele imparts a growth restriction similar to that seen with complete deletions of the ICP22 gene (51). *d*95 titers are reduced 5- to 10-fold relative to *d*92 titers (data not shown). Also, the region of ICP22 that is most conserved among the herpesviruses (25, 51) is excluded by virtue of the *n*199 mutation. An additional unlikely possibility is that a fortuitous gain-of-function mutation contributes to the phenotype of *d*95.

In the absence of ICP4, ICP27, and ICP22, cell DNA synthesis was inhibited and ICP0 accumulated to very high levels in discrete structures in the nucleus. The formation of large nuclear inclusions correlated with the absence of ICP27. This finding may reflect previous observations that the expression of ICP27 in the absence of ICP4 results in the cytoplasmic localization of ICP0 (81, 82). Also of note is the observation that the expression of ICP22 results in the formation of fine granular structures in the nucleus. In the presence of nuclear ICP0, as in *d*92, these appeared to coalesce around the ICP0-containing bodies (Fig. 8D). This finding raises the possibility that molecules present as a function of ICP22 interact with ICP0. Further studies on the identities and compositions of the ICP22-dependent structures will be necessary to address this question.

The observations described in this study reflect some of the effects of the IE proteins on host cell metabolism. Presumably some of these changes occur early in the viral infection and prime the infected cell for productive viral infection. It is also possible that some of the observed effects are exaggerated or are a consequence of IE protein overexpression. In either case, these results also bear on the use of IE deletion mutants of HSV for use as gene transfer vehicles. While viral backgrounds such as *d*95 may have utility in some cases or in certain cell types, it is highly likely that all of the regulatory IE genes are deleterious to host cell survival and that they will all have to be deleted if HSV is to be generally used as a vector.

ACKNOWLEDGMENTS

This work was supported by NIH grants AI30612, DK44935, and CA20260.

REFERENCES

1. **Alwine, J., W. Stein, and C. Hill.** 1974. Transcription of herpes simplex type 1 DNA in nuclei isolated from infected Hep-2 and KB cells. Virology **60:** 302–307.
2. **Ascoli, C. A., and G. G. Maul.** 1991. Identification of a novel nuclear domain. J. Cell Biol. **112:**785–795.
3. **Batterson, W., and B. Roizman.** 1983. Characterization of the herpes simplex virion-associated factor responsible for the induction of alpha genes. J. Virol. **46:**371–377.

3a. **Biotecx.** 1992. Bulletin 27. Biotecx, Houston, Tex.

4. **Bohenzky, R. A., A. G. Papavassiliou, I. H. Gelman, and S. Silverstein.** 1993. Identification of a promoter mapping within the reiterated sequences that flank the herpes simplex virus type 1 U_L region. J. Virol. **67:**632–642.
5. **Bond, J. F., G. S. Robinson, and S. R. Farmer.** 1984. Differential expression of two neural cell-specific β-tubulin mRNAs during rat brain development. Mol. Cell. Biol. **4:**1313–1319.
6. **Cai, W., T. L. Astor, L. M. Liptak, C. Cho, D. M. Coen, and P. A. Schaffer.** 1993. The herpes simplex virus type 1 regulatory protein ICP0 enhances virus replication during acute infection and reactivation from latency. J. Virol. **67:**7501–7512.
7. **Cai, W., and P. A. Schaffer.** 1992. Herpes simplex virus type 1 ICP0 regulates expression of immediate-early, early, and late genes in productively infected cells. J. Virol. **66:**2904–2915.
8. **Campbell, M. E., J. W. Palfreyman, and C. M. Preston.** 1984. Identification of herpes simplex virus DNA sequences which encode a trans-acting polypeptide responsible for stimulation of immediate early transcription. J. Mol. Biol. **180:**1–19.
9. **Chapman, C. J., J. D. Harris, M. A. Hardwicke, R. M. Sandri-Goldin, M. K. Collins, and D. S. Latchman.** 1992. Promoter independent activation of heterologous virus gene expression by the herpes simplex virus immediate-early protein ICP27. Virology **186:**573–578.
10. **Clements, J. B., R. J. Watson, and N. M. Wilkie.** 1977. Temporal regulation of herpes simplex virus type 1 transcription: location of transcripts on the viral genome. Cell **12:**275–285.
11. **DeLuca, N. A., A. M. McCarthy, and P. A. Schaffer.** 1985. Isolation and characterization of deletion mutants of herpes simplex virus type 1 in the gene encoding immediate-early regulatory protein ICP4. J. Virol. **56:**558–570.
12. **DeLuca, N. A., and P. A. Schaffer.** 1985. Activation of immediate-early, early, and late promoters by temperature-sensitive and wild-type forms of herpes simplex virus type 1 protein ICP4. Mol. Cell. Biol. **5:**1997–2208.
13. **DeLuca, N. A., and P. A. Schaffer.** 1987. Activities of herpes simplex virus type 1 (HSV-1) ICP4 genes specifying nonsense peptides. Nucleic Acids Res. **15:**4491–4511.
14. **Dixon, R. A., and P. A. Schaffer.** 1980. Fine-structure mapping and functional analysis of temperature-sensitive mutants in the gene encoding the herpes simplex virus type 1 immediate early protein VP175. J. Virol. **36:**189–203.
15. **Dyck, J. A., G. G. Maul, W. H. Miller, Jr., J. D. Chen, A. Kakizuka, and R. M. Evans.** 1994. A novel macromolecular structure is a target of the promyelocyte-retinoic acid receptor oncoprotein. Cell **76:**333–343.
16. **Everett, R. D.** 1984. Trans activation of transcription by herpes virus products: requirement for two HSV-1 immediate-early polypeptides for maximum activity. EMBO J. **3:**3135–3141.
17. **Everett, R. D., and G. G. Maul.** 1994. HSV-1 IE protein Vmw110 causes redistribution of PML. EMBO J. **13:**5062–5069.
18. **Gelman, I. H., and S. Silverstein.** 1985. Identification of immediate early genes from herpes simplex virus that transactivate the virus thymidine kinase gene. Proc. Natl. Acad. Sci. USA **82:**5265–5269.
19. **Gerster, T., and R. G. Roeder.** 1988. A herpesvirus trans-activating protein interacts with transcription factor OTF-1 and other cellular proteins. Proc. Natl. Acad. Sci. USA **85:**6347–6351.
20. **Goding, C. R., and P. O'Hare.** 1989. Herpes simplex virus Vmw65-octamer binding protein interaction: a paradigm for combinatorial control of transcription. Virology **173:**363–367.
21. **Greaves, R., and P. O'Hare.** 1989. Separation of requirements for protein-DNA complex assembly from those for functional activity in the herpes simplex virus regulatory protein Vmw65. J. Virol. **63:**1641–1650.
22. **Gu, B., R. Rivera-Gonzalez, C. A. Smith, and N. A. DeLuca.** 1993. Herpes simplex virus infected cell polypeptide 4 preferentially represses Sp1-activated over basal transcription from its own promoter. Proc. Natl. Acad. Sci. USA **90:**9528–9532.
23. **Hardwicke, M. A., and R. M. Sandri-Goldin.** 1994. The herpes simplex virus regulatory protein ICP27 contributes to the decrease in cellular mRNA levels during infection. J. Virol. **68:**4797–4810.
24. **Hardy, W. R., and R. M. Sandri-Goldin.** 1994. Herpes simplex virus inhibits host cell splicing, and regulatory protein ICP27 is required for this effect. J. Virol. **68:**7790–7799.
25. **Holden, V. R., R. R. Yalamanchili, R. N. Harty, and D. J. O'Callaghan.** 1992. ICP22 homolog of equine herpesvirus 1: expression from early and late promoters. J. Virol. **66:**664–673.
26. **Honess, R. W., and B. Roizman.** 1974. Regulation of herpesvirus macromolecular synthesis. I. Cascade regulation of the synthesis of three groups of viral proteins. J. Virol. **14:**8–19.
27. **Honess, R. W., and B. Roizman.** 1975. Regulation of herpesvirus macromolecular synthesis: sequential transition of polypeptide synthesis requires functional viral polypeptides. Proc. Natl. Acad. Sci. USA **72:**1276–1280.
28. **Imbalzano, A. N., D. Coen, and N. A. DeLuca.** 1991. Herpes simplex virus transactivator ICP4 operationally substitutes for the cellular transcription factor Sp1 for efficient expression of the viral thymidine kinase gene. J. Virol. **65:**565–574.
29. **Johnson, P. A., A. Miyanohara, F. Levine, T. Cahill, and T. Friedmann.** 1992. Cytotoxicity of a replication-defective mutant of herpes simplex virus type 1. J. Virol. **66:**2952–2965.
30. **Johnson, P. A., M. J. Wang, and T. Friedmann.** 1994. Improved cell survival by the reduction of immediate-early gene expression in replication-defective mutants of herpes simplex virus type 1 but not by mutation of the virion host shutoff function. J. Virol. **68:**6347–6362.
31. **Knipe, D. M., and J. L. Smith.** 1986. A mutant herpesvirus protein leads to a block in nuclear localization of other viral proteins. Mol. Cell. Biol. **6:**2371–2381.
32. **Koken, M. H., F. Puvion-Dutilleul, M. C. Guillemin, A. Viron, G. Linares-Cruz, N. Stuurman, L. de Jong, C. Szostecki, F. Calvo, C. Chomienne, L. Degos, E. Puvion, and H. de The.** 1994. The t (15;17) translocation alters a nuclear body in a retinoic acid-reversible fashion. EMBO J. **13:**1073–1083.
33. **Kristie, T. M., J. H. LeBowitz, and P. A. Sharp.** 1989. The octamer-binding proteins form multi-protein—DNA complexes with the HSV alpha TIF regulatory protein. EMBO J. **8:**4229–4238.
34. **Lagunoff, M., and B. Roizman.** 1994. Expression of a herpes simplex virus 1 open reading frame antisense to the $\gamma_1$34.5 gene and transcribed by an RNA 3′ coterminal with the unspliced latency-associated transcript. J. Virol. **68:** 6021–6028.
35. **Lagunoff, M., and B. Roizman.** 1995. The regulation of synthesis and prop-

erties of the protein product of open reading frame P of the herpes simplex virus 1 genome. J. Virol. **69:**3615–3623.
36. **Lee, M. G., S. A. Lewis, C. D. Wilde, and N. J. Cowan.** 1983. Evolutionary history of a multigene family and expressed human β-tubulin gene and three processed pseudogenes. Cell **33:**477–487.
37. **Leib, D. A., D. M. Coen, C. L. Bogard, K. A. Hicks, D. R. Yager, D. M. Knipe, K. L. Tyler, and P. A. Schaffer.** 1989. Immediate-early regulatory mutants define stages in the establishment and reactivation of herpes simplex virus latency. J. Virol. **63:**759–768.
38. **Maul, G. G., and R. D. Everett.** 1994. The nuclear location of PML, a cellular member of the C3HC4 zinc-binding domain protein family, is rearranged during herpes simplex virus infection by the C3HC4 viral protein ICP0. J. Gen. Virol. **75:**1223–1233.
39. **McCarthy, A. M., L. McMahan, and P. A. Schaffer.** 1989. Herpes simplex virus type 1 ICP27 deletion mutants exhibit altered patterns of transcription and are DNA deficient. J. Virol. **63:**18–27.
40. **McGeoch, D. J., M. A. Dalrymple, A. J. Davison, A. Dolan, M. C. Frame, D. McNab, L. J. Perry, J. E. Scott, and P. Taylor.** 1988. The complete sequence of the long unique region in the genomes of herpes simplex virus type 1. J. Gen. Virol. **69:**1531–1574.
41. **McGeoch, D. J., A. Dolan, S. Donald, and F. J. Rixon.** 1985. Sequence determination and genetic content of the short unique region in the genome of herpes simplex virus type 1. J. Mol. Biol. **181:**1–13.
42. **McLauchlan, J., A. Phelan, C. Loney, R. M. Sandri-Goldin, and J. B. Clements.** 1992. Herpes simplex virus IE63 acts at the posttranscriptional level to stimulate viral mRNA 3′ processing. J. Virol. **66:**6939–6945.
43. **McLauchlan, J., S. Simpson, and J. B. Clements.** 1989. Herpes simplex virus induces a processing factor that stimulates poly(A) site usage. Cell **59:**1093–1105.
44. **McMahan, L., and P. A. Schaffer.** 1990. The repressing and enhancing functions of the herpes simplex virus regulatory protein ICP27 map to C-terminal regions and are required to modulate viral gene expression very early in infection. J. Virol. **64:**3471–3485.
45. **Michael, N., and B. Roizman.** 1993. Repression of the herpes simplex virus 1 alpha 4 gene by its gene product occurs within the context of the viral genome and is associated with all three identified cognate sites. Proc. Natl. Acad. Sci. USA **90:**2286–2290.
46. **O'Hare, P., C. R. Goding, and A. Haigh.** 1988. Direct combinatorial interaction between a herpes simplex virus regulatory protein and a cellular octamer-binding factor mediates specific induction of virus immediate-early gene expression. EMBO J. **7:**4231–4238.
47. **O'Hare, P., and G. S. Hayward.** 1985. Evidence for a direct role for both the 175,000- and 110,000-molecular-weight immediate-early proteins of herpes simplex virus in the transactivation of delayed-early promoters. J. Virol. **53:**751–760.
48. **O'Hare, P., and G. S. Hayward.** 1985. Three *trans*-acting regulatory proteins of herpes simplex virus modulate immediate-early gene expression in a pathway involving positive and negative feedback regulation. J. Virol. **56:**723–733.
49. **Peat, D. S., and M. A. Stanley.** 1986. Chromosomal damage induced by herpes simplex virus type 1 in early infection. J. Gen. Virol. **67:**2273–2277.
50. **Pereira, L., M. H. Wolff, M. Fenwick, and B. Roizman.** 1977. Regulation of herpesvirus macromolecular synthesis. V. Properties of alpha polypeptides made in HSV-1 and HSV-2 infected cells. Virology **77:**733–749.
51. **Poffenberger, K. L., P. E. Raichlen, and R. C. Herman.** 1993. In vitro characterization of a herpes simplex virus type 1 ICP22 deletion mutant. Virus Genes **7:**171–186.
52. **Preston, C. M.** 1979. Control of herpes simplex virus type 1 mRNA synthesis in cells infected with wild-type virus or the temperature-sensitive mutant *tsK*. J. Virol. **29:**275–284.
53. **Quinlan, M. P., and D. M. Knipe.** 1985. Stimulation of expression of a herpes simplex virus DNA-binding protein by two viral functions. Mol. Cell. Biol. **5:**957–963.
53a. **Read, G. S., and N. Frenkel.** 1983. Herpes simplex virus mutants defective in the virion-associated shutoff of host polypeptide synthesis and exhibiting abnormal synthesis of α (immediate early) viral polypeptides. J. Virol. **46:**498–512.
54. **Rice, S. A., and D. M. Knipe.** 1988. Gene-specific transactivation by herpes simplex virus type 1 alpha protein ICP27. J. Virol. **62:**3814–3823.
55. **Rice, S. A., M. C. Long, V. Lam, P. A. Schaffer, and C. A. Spencer.** 1995. Herpes simplex virus immediate-early protein ICP22 is required for viral modification of host RNA polymerase II and establishment of the normal viral transcription program. J. Virol. **69:**5550–5559.
56. **Roberts, M. S., A. Boundy, P. O'Hare, M. C. Pizzorno, D. M. Ciufo, and G. S. Hayward.** 1988. Direct correlation between a negative autoregulatory response element at the cap site of the herpes simplex virus type 1 IE175 (alpha 4) promoter and a specific binding site for the IE175 (ICP4) protein. J. Virol. **62:**4307–4320.
57. **Sacks, W. R., C. C. Greene, D. P. Aschman, and P. A. Schaffer.** 1985. Herpes simplex virus type 1 ICP27 is an essential regulatory protein. J. Virol. **55:**796–805.
58. **Sacks, W. R., and P. A. Schaffer.** 1987. Deletion mutants in the gene encoding the herpes simplex virus type 1 immediate-early protein ICP0 exhibit impaired growth in cell culture. J. Virol. **61:**829–839.
59. **Samaniego, L. A., A. L. Webb, and N. A. DeLuca.** 1995. Functional interactions between herpes simplex virus immediate-early proteins during infection: gene expression as a consequence of ICP27 and different domains of ICP4. J. Virol. **69:**5705–5715.
60. **Sambrook, J., E. F. Fritsch, and T. Maniatis.** 1989. Molecular cloning: a laboratory manual, 2nd ed. Cold Spring Harbor Laboratory Press, Cold Spring Harbor, N.Y.
61. **Sandri-Goldin, R. M.** 1994. Properties of an HSV-1 regulatory protein that appears to impair host cell splicing. Infect. Agents Dis. **3:**59–67.
62. **Sandri-Goldin, R. M., M. K. Hibbard, and M. A. Hardwicke.** 1995. The C-terminal repressor region of herpes simplex virus type 1 ICP27 is required for the redistribution of small nuclear ribonucleoprotein particles and splicing factor SC35; however, these alterations are not sufficient to inhibit host cell splicing. J. Virol. **69:**6063–6076.
63. **Sandri-Goldin, R. M., and G. E. Mendoza.** 1992. A herpesvirus regulatory protein appears to act post-transcriptionally by affecting mRNA processing. Genes Dev. **6:**848–863.
64. **Schwyzer, M., U. V. Wirth, B. Vogt, and C. Fraefel.** 1994. BICP22 of bovine herpesvirus 1 is encoded by a spliced 1.7 kb RNA which exhibits immediate early and late transcription kinetics. J. Gen. Virol. **75:**1703–1711.
65. **Sears, A. E., I. W. Halliburton, B. Meignier, S. Silver, and B. Roizman.** 1985. Herpes simplex virus 1 mutant deleted in the alpha 22 gene: growth and gene expression in permissive and restrictive cells and establishment of latency in mice. J. Virol. **55:**338–346.
66. **Sekulovich, R. E., K. Leary, and R. M. Sandri-Goldin.** 1988. The herpes simplex virus type 1 alpha protein ICP27 can act as a *trans*-repressor or a *trans*-activator in combination with ICP4 and ICP0. J. Virol. **62:**4510–4522.
67. **Smith, C. A., P. Bates, R. Rivera-Gonzalez, B. Gu, and N. A. DeLuca.** 1993. ICP4, the major transcriptional regulatory protein of herpes simplex virus type 1, forms a tripartite complex with TATA-binding protein and TFIIB. J. Virol. **67:**4676–4687.
68. **Smith, I. L., M. A. Hardwicke, and R. M. Sandri-Goldin.** 1992. Evidence that the herpes simplex virus immediate early protein ICP27 acts post-transcriptionally during infection to regulate gene expression. Virology **186:**74–86.
69. **Southern, E. M.** 1975. Detection of specific sequences among DNA fragments separated by gel electrophoresis. J. Mol. Biol. **98:**503–517.
70. **Su, L., and D. M. Knipe.** 1989. Herpes simplex virus alpha protein ICP27 can inhibit or augment viral gene transactivation. Virology **170:**496–504.
71. **Triezenberg, S. J., K. L. LaMarco, and S. L. McKnight.** 1988. Evidence of DNA: protein interactions that mediate HSV-1 immediate early gene activation by VP16. Genes Dev. **2:**730–742.
72. **Uprichard, S. L., and D. M. Knipe.** 1996. Herpes simplex ICP27 mutant viruses exhibit reduced expression of specific DNA replication genes. J. Virol. **70:**1969–1980.
73. **Watson, R. J., and J. B. Clements.** 1978. Characterization of transcription-deficient temperature-sensitive mutants of herpes simplex virus type 1. Virology **91:**364–379.
74. **Watson, R. J., C. M. Preston, and J. B. Clements.** 1979. Separation and characterization of herpes simplex virus type 1 immediate-early mRNA's. J. Virol. **31:**42–52.
75. **Weis, K., S. Rambaud, C. Lavau, J. Jansen, T. Carvalho, M. Carmo-Fonseca, A. Lamond, and A. Dejean.** 1994. Retinoic acid regulates aberrant nuclear localization of PML-RAR alpha in acute promyelocytic leukemia cells. Cell **76:**345–356.
76. **Weller, S. K., D. P. Aschman, W. R. Sacks, D. M. Coen, and P. A. Schaffer.** 1983. Genetic analysis of temperature-sensitive mutants of HSV-1: the combined use of complementation and physical mapping for cistron assignment. Virology **130:**290–305.
77. **Wilcox, K. W., A. Kohn, E. Sklyanskaya, and B. Roizman.** 1980. Herpes simplex virus phosphoproteins. I. Phosphate cycles on and off some viral polypeptides and can alter their affinity for DNA. J. Virol. **33:**167–182.
78. **Xie, K., E. J. Lambie, and M. Snyder.** 1993. Nuclear dot antigens may specify transcriptional domains in the nucleus. Mol. Cell. Biol. **13:**6170–6179.
79. **Yeh, L., and P. A. Schaffer.** 1993. A novel class of transcripts expressed with late kinetics in the absence of ICP4 spans the junction between the long and short segments of the herpes simplex virus type 1 genome. J. Virol. **67:**7373–7382.
80. **York, I. A., C. Roop, D. W. Andrews, S. R. Riddell, F. L. Graham, and D. C. Johnson.** 1994. A cytosolic herpes simplex virus protein inhibits antigen presentation to CD8+ T lymphocytes. Cell **77:**525–535.
81. **Zhu, Z., W. Cai, and P. A. Schaffer.** 1994. Cooperativity among herpes simplex virus type 1 immediate-early regulatory proteins: ICP4 and ICP27 affect the intracellular localization of ICP0. J. Virol. **68:**3027–3040.
82. **Zhu, Z., N. DeLuca, and P. A. Schaffer.** 1996. Overexpression of the herpes simplex virus type 1 immediate-early regulatory protein, ICP27, is responsible for the aberrant localization of ICP0 and mutant forms of ICP4 in ICP4 mutant virus-infected cells. J. Virol. **70:**5346–5356.